



HAL
open science

Simulating record-shattering cold winters of the 21st century in France

Camille Cadiou, Pascal Yiou

► **To cite this version:**

Camille Cadiou, Pascal Yiou. Simulating record-shattering cold winters of the 21st century in France. 2022. hal-03900209v1

HAL Id: hal-03900209

<https://hal.science/hal-03900209v1>

Preprint submitted on 15 Dec 2022 (v1), last revised 29 Feb 2024 (v2)

HAL is a multi-disciplinary open access archive for the deposit and dissemination of scientific research documents, whether they are published or not. The documents may come from teaching and research institutions in France or abroad, or from public or private research centers.

L'archive ouverte pluridisciplinaire **HAL**, est destinée au dépôt et à la diffusion de documents scientifiques de niveau recherche, publiés ou non, émanant des établissements d'enseignement et de recherche français ou étrangers, des laboratoires publics ou privés.

1 **Simulating record-shattering cold**
2 **winters of the 21st century in France**

3 Camille Cadiou ^{*a} and Pascal Yiou^a

4 ^aLaboratoire des Sciences du Climat et de l'Environnement, UMR 8212
5 CEA-CNRS-UVSQ, IPSL and U Paris Saclay, 91191 Gif-sur-Yvette CEDEX,
6 France

7 December 2022

*Corresponding Author

camille.cadiou@lsce.ipsl.fr

Extreme winter cold temperatures in Europe have huge societal impacts on society. Being able to simulate worst-case scenarios of such events for present and future climates is hence crucial for short and long-term adaptation. In this paper, we are interested in low probability cold events, whose probability is deemed to decrease with climate change. Rather than simulating very large ensembles of normal climate trajectories, rare event algorithms allow sampling the tail of distributions in an efficient way. Such algorithms have been applied to simulate extreme heat waves. They have emphasized the role of atmospheric circulation in such extremes. The goal of this study is to evaluate the dynamics of extreme cold spells simulated by a rare event algorithm. We focus first on winter cold temperatures that have occurred in France from 1950 to 2021. We investigate winter mean temperatures in France (December, January, and February) and identify a record-shattering event in 1963. We find that, although the frequency of extreme cold spells decreases with time, their intensity is stationary. We applied a stochastic weather generator approach with importance sampling, to simulate the coldest winters that could occur every year since 1950. We hence simulated ensembles of worst winter cold spells that are consistent with reanalyses. We find that a few simulations reach colder temperatures than the record-shattering event of 1963. The atmospheric circulation that prevails during those events is analyzed and compared to the observed circulation during the record-breaking events.

1 Introduction

Winter cold spells in the mid latitudes have had wide-ranging impacts, affecting agriculture (Trnka et al., 2011; Vogel et al., 2019), health (Gasparrini et al., 2015; Smith and Sheridan, 2019), infrastructures (Chang et al., 2007), or energy systems (Añel et al., 2017; Bessec and Fouquau, 2008; Van Der Wiel et al., 2019). Cold events are expected to decrease both in terms of intensity and frequency with climate change in most regions of the world (Seneviratne et al., 2021), which could lead to a reduction of their impacts. In the last decades a decrease in intensity has been recorded in the Western European region (Cattiaux et al., 2010; Seneviratne et al., 2021; Smith and Sheridan, 2020; Van Oldenborgh et al., 2019). But even if their probability decreases, extreme cold winter events still occur and can cause major disruptions, like winter 2010 in Western Europe (Cattiaux et al., 2010) or the cold snap of February 2021 in Texas (Doss-Gollin et al., 2021). Winter 2010 was perceived as extremely cold in Europe and rose questions in the media and general public about

39 the occurrence of extreme cold events under climate change. Cattiaux et al. (2010) showed that
40 winter 2010 was actually not as extreme as records of the previous decades and would have been
41 much more extreme given the same atmospheric conditions if it had occurred in a past climate with
42 a lower influence of climate change. This is consistent with the general upward trend of winter
43 minimum temperatures as shown in Fig. 1a.

44 However, uncertainties remain about the potential dynamical effects of climate change on
45 severe winter mid-latitudes weather (Cohen et al., 2020; Horton et al., 2015; Overland et al., 2016;
46 Shepherd, 2015). The Arctic Amplification (AA) is a mechanism that may lead to an increase in
47 severe winter weather in the mid-latitudes (Cohen et al., 2014; Francis et al., 2018; Francis and
48 Vavrus, 2012; Vavrus, 2018). But its potential effect is intertwined with other hemispheric drivers
49 of decadal variability and the quantification of its influence remains debated (Blackport and Screen,
50 2020; Cohen et al., 2020; Francis, 2017). Several studies have also shown that winter warming and
51 winter anomalies trends are not as large as the upward trend of summer warm anomalies in the
52 northern hemisphere (Robeson et al., 2014) and more specifically in France (Ribes et al., 2022). The
53 decrease in winter cold spells would consequently not be as significant as the increase in summer
54 heat waves.

55 To assess worst case scenario winter temperatures in France, we use the winter 1962-1963
56 as a reference event. Winter 1963 yielded an exceptionally low mean temperature anomaly over
57 December, January and February (DJF) of -3.4σ (Fig. 1a). 1963 was also extreme by its spatial
58 scale, with negative temperatures covering most of Europe (Greatbatch et al., 2015; Hirschi and
59 Sinha, 2007; O’connor, 1963). This led to exceptional weather across the continent: large lakes,
60 like Lake Constance or Lake Zurich, froze entirely and widespread and persistent snow coverage was
61 observed in the British Isles. According to the Met office, it was the coldest winter since 1740 in
62 the United Kingdom. In France, a first intense cold wave occurred at the end of December, lasting
63 one week, followed by a second more prolonged cold wave with negative daily mean temperature
64 over France from the 11th of January to the 6th of February (Fig. 1b). Winter 1962-1963 was
65 associated with a negative North Atlantic Oscillation (NAO) index, indicating lower than normal
66 pressure difference between the Iceland low and Azores high-pressure systems (Cattiaux et al.,
67 2010; Greatbatch et al., 2015). A persistent negative NAO phase is usually associated with the
68 development of North-Atlantic atmospheric blockings (Shabbar et al., 2001), and a weakening of
69 the westerlies allowing outbreaks of cold air coming from the Arctic or Russia into Western Europe

70 (Greatbatch, 2000; Hurrell et al., 2003).

71 According to the definition of Fischer et al. (2021), winter 1963 was a record-shattering event
72 in France, i.e. the record of low temperatures was broken with a large margin of several standard
73 deviations (Fig. 1a). Therefore, winter 1962-1963 was an extremely low probability event, even
74 considering the colder climate (than in the 21st century) in which it occurred. If the average winter
75 temperature follows a Gaussian distribution, this corresponds to a return period larger than 10^3
76 years, which is longer than observational periods. The objective of this study is to examine whether
77 such a winter is still possible in the 21st century, considering the warmer climate in western Europe
78 in present times.

79 Simulating ensemble of events whose return period is larger than the observational period,
80 or the typical length of climate model simulations (e.g. ≈ 200 years for CMIP6 (Eyring et al.,
81 2016)) requires intensive computing resources. Several methods based on principles of statistical
82 physics have been developed to provide fast and realistic simulations of large values of atmospheric
83 variables. Rare events algorithm using importance sampling (e.g. Ragone and Bouchet, 2021) have
84 been designed to specifically simulated extreme heat waves from a climate model. An alternative
85 approach is based on Stochastic Weather Generators (SWG). SWGs are Markov processes used to
86 generate large ensembles of atmospheric trajectories with realistic statistical properties, at a low
87 computational cost (Ailliot et al., 2015). Yiou and Déandréis (2019) combined an SWG based on
88 analogs of circulation developed by (Yiou, 2014) and the importance sampling principle exposed in
89 (Ragone and Bouchet, 2021) to specifically simulate extreme summer heat waves from analogs of
90 circulation. This method allows to simulate ensemble of physically consistent trajectories of extreme
91 events at a very low computational cost. In this study, we adapt the analog-based stochastic weather
92 generator with importance sampling of Yiou and Déandréis (2019) to the simulation of extreme cold
93 winter events.

94 We use SWG simulations based on reanalysis data in order to assess the intensity of the
95 worst-case winter scenario in France in a counterfactual period (with lower influence of climate
96 change) and a factual period representing the present-day climate with more detectable influence of
97 climate change. Therefore, we examine how climate change affects the intensity of worst case cold
98 winters that can hit France.

99 The paper is organized as follows. Section 2 presents the datasets used in the paper and

100 details the analog-based stochastic weather generator model for sampling cold winters. Section 3
 101 shows the results of the simulations of extreme winters. Section 4 discusses the main results of the
 102 study.

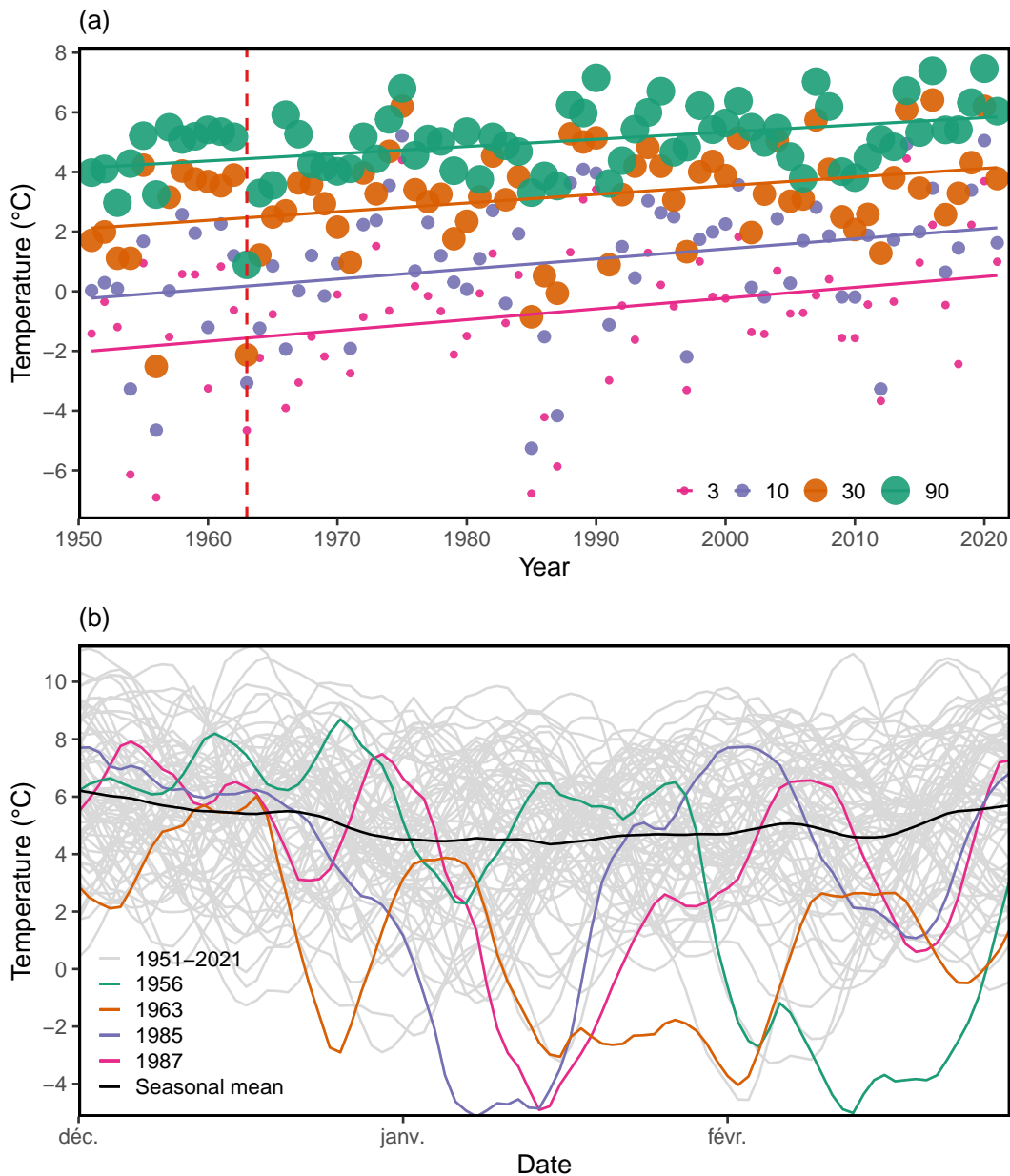


Figure 1: (a) Minimum of winter temperatures over DJF for four time scales in continental France. For each winter we compute the n -day running mean of daily mean temperature for $n \in \{3, 10, 30, 90\}$ days and select the minimum value. The colored lines are linear regressions of the temperature averages. The vertical dashed line outlines 1963 (coldest winter in France). (b) Time series of DJF 7-days running mean temperature at 2m from 1950-1951 to 2020-2021 in continental France. The curves in colour are for the four coldest years (1956, 1963, 1985 and 1987) and the black curve is for the seasonal mean computed over 1951-2021.

103 2 Data and Methods

104 2.1 Data

105 Daily mean surface temperature ($t2m$) data were obtained from the 5th version (ERA5) of the
106 atmospheric reanalysis of the European Centre for Medium-Range Weather Forecasts (ECMWF)
107 (Hersbach et al., 2020). Data from 1950 to 2021 has been retrieved with a spatial resolution of
108 $0.25^\circ \times 0.25^\circ$. Daily temperature fields were averaged over the smallest spatial domain including
109 metropolitan France ($5^\circ\text{W} - 9^\circ\text{E}$; $42^\circ\text{N} - 52^\circ\text{N}$). ERA5 was chosen for its large time coverage and
110 its high horizontal resolution of 0.25° .

111 We compute running averages of temperature for four time scales ($r = 3, 10, 30$ and 90 days)
112 and determine the minimum value for each winter (from December to February). This corresponds
113 to identifying the coldest r -day period for each year, or $\text{TN}r\text{d}$. Fig. 1a shows the variations of
114 $\text{TN}r\text{d}$ time series for France. We observe a upward trends of $\text{TN}r\text{d}$ at the four time scales r . The
115 records at each time scale occurred before 1990. However, extreme cold events still happened in
116 the 21st century: winter 2012 witnessed the 5th coldest 10-day and the 8th coldest 3-day cold
117 spells of the 1950-2021 period. At the 30-day time scale, February 1956 and January 1963 were
118 two very extreme events, with temperature anomalies to the 1950-2021 trend of respectively -2.9σ
119 and -2.8σ . One event really stands out in the 90-day winter temperatures: winter 1963 is at 3.7σ
120 from the trend of winter mean temperatures and 2.2σ under the second coldest winter in 1950-2021,
121 winter 1952-1953. For conciseness, this paper focuses on $\text{TN}90\text{d}$, i.e. DJF average temperatures.

122 For the computation of analogs of circulation, we use daily geopotential height at 500 hPa
123 ($Z500$) from ERA5 reanalysis from 1950 to 2021. $Z500$ was chosen over SLP because of its lower
124 sensibility to perturbations from the surface roughness and its common use on weather regime
125 studies (Corti et al., 1999; Yiou and Nogaj, 2004; Jézéquel et al., 2018; Dawson et al., 2012).
126 Jézéquel et al. (2018) also showed it was better suited to simulate temperature anomalies, although
127 that study investigated warm temperatures. $Z500$ data were regridded on a $1^\circ \times 1^\circ$ grid to reduce
128 computation time since a higher resolution has little impact on the analogs calculation because of the
129 smooth spatial variability of $Z500$ fields. We considered the $Z500$ field over the North Atlantic region
130 ($20^\circ\text{W} - 30^\circ\text{E}$; $30^\circ\text{N} - 70^\circ\text{N}$) to compute circulation analogs. This domain offers a compromise
131 between a spatial coverage large enough to study the role of the synoptic circulation but small

132 enough not to drown out the signal in the too complex hemispheric circulation.

133 **2.2 Methods: Analogs of circulation**

134 We first compute a database of analogs of circulation following the procedure of (Yiou and
135 Jézéquel, 2020). For a given day t , we compute the Euclidean distance of the Z500 fields between
136 t and all days t' that are not in the same year or season (astride two following years) and within
137 a calendar distance to t inferior to 30 days. The K analogs days of t are the K days for which
138 the distance from t is the smallest. We chose $K = 20$ analogs, as advocated in previous studies
139 (Krouma et al., 2022; Platzer et al., 2021).

140 The circulation analogs were computed using the "Blackswan" Web Processing Service
141 (Hempelmann et al., 2018). We consider three different analog data sets, depending on the time
142 period in which the analogs are selected:

- 143 1. 1950-2021: the whole length of available ERA5 data,
- 144 2. 1950-1999: the past period, as a counterfactual, with less influence of anthropogenic climate
145 change.
- 146 3. 1972-2021: the present period, as a factual, with a significant signal from climate change.

147 The analog periods were chosen to have sufficient length to be representative of all the possible
148 states of the atmospheric patterns while being characteristic of climate periods that are significantly
149 different. We were constrained by the length of the ERA5 data available (only 71 years). Therefore
150 we chose a compromise between analog depth and low overlap by considering two 50-year periods
151 (1950-1999 and 1972-2021).

152 **2.3 Methods: Stochastic Weather Generator and importance sampling**

153 The analog-based stochastic weather generator (hereafter referred as SWG) developed by
154 Yiou (2014) uses stochastic reshuffling of daily atmospheric fields to generate atmospherically-
155 consistent alternative trajectories of climate events. This algorithm was adapted by Yiou and
156 Jézéquel (2020) to simulate extreme heat waves using a principle of importance sampling. The goal
157 is to simulate L day trajectories of a model while optimizing an observable. Here, the observable
158 is the average temperature over France. For simplicity, this paper focuses on $L = 90$ day events,
159 starting on a 1st of December, i.e. the whole winter (December-January-February).

160 Here we focus on the so-called "dynamic" type of simulations, developed by Yiou (2014),
 161 which computes alternative atmospheric trajectories starting with the same initial conditions as an
 162 observed event. We start at an initial condition t_0 . To simulate temperature for the day after t_0
 163 ($t = t_0 + 1$), we randomly pick one analog among the K best analogs of t . This analog day is
 164 the simulated day t' . For the next time step, t is replaced by $t' + 1$, the day following t' . This
 165 random process is repeated sequentially for L time steps, the length of the simulation. This defines
 166 a Markov chain with hidden states provided by the analogs of Z500.

167 At each time step, the selection of the analog day follows several constraints and weights
 168 controlled by the parameters that are described hereafter. To better follow the seasonal cycle of
 169 the simulated season, we use K weights $\omega_{cal}^{(k)}$ ($k \in \{1, \dots, K\}$) on the analog selection that depend
 170 on a parameter α_{cal} which favours analog days that are closest to the calendar date of time step t :

$$171 \quad \omega_{cal}^{(k)} = A_{cal} e^{-\alpha_{cal} d_k} \quad (1)$$

172 where A_{cal} is a normalizing constant, $\alpha_{cal} \geq 0$ is the calendar weight and d_k is the number of calendar
 173 days between the k^{th} analog day and t . We simulated ensembles of trajectories of 90 days starting
 174 on Dec. 1st of each year, with different values of parameter α_{cal} . Figure 2a shows the percentage of
 175 simulations for which the last day of the simulations falls after the 15th of February. With too low
 176 calendar weight (e.g. $\alpha_{cal} = 1$), fewer than half of the simulations end with a calendar day after the
 177 15th of February. This means that the trajectories of the simulated events with $\alpha_{cal} = 1$ are less
 178 consistent with the seasonal cycle. With an α_{cal} parameter greater than 5, more than 75% of the
 179 simulations have their last day falling after the 15th of February. Therefore we use $\alpha_{cal} = 5$ in the
 180 following.

181 To favour the simulation of the most extreme events, importance sampling weights $\omega_T^{(k)}$ are
 182 introduced, with a control parameter $\alpha_T \geq 0$. The higher α_T , the more the stochastic weather gen-
 183 erator favours analog days with extreme temperatures. The K analogs of t are sorted in ascending
 184 order of temperature with ranks R_k ($k \in \{1, \dots, K\}$), so that the coldest analog day has a rank of
 185 1. Hence the weight associated to the k^{th} analog day of t is:

$$186 \quad \omega_T^{(k)} = A_T e^{-\alpha_T R_k} \quad (2)$$

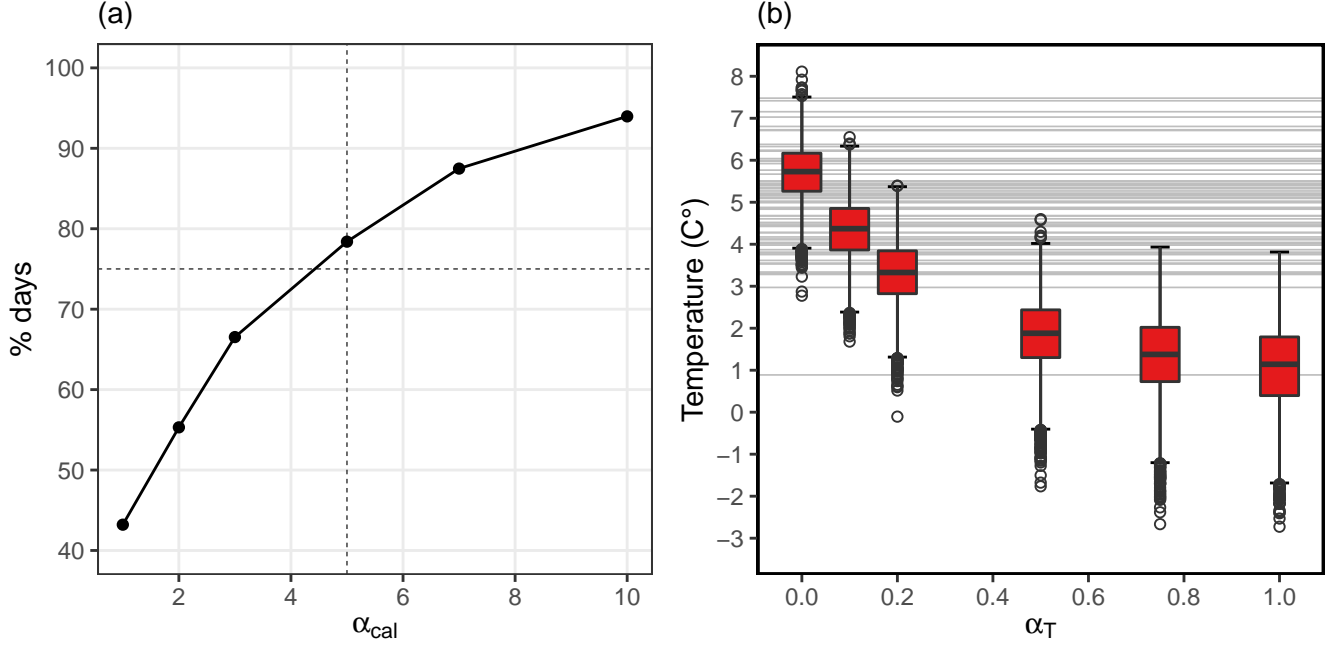


Figure 2: (a) Percentage of simulations of extreme winters for which the last day falls after the 15th of February, as a function of the α_{cal} parameter. (b) Temperature distribution of 100 simulations (method 2) for each winter between 1950-1951 and 2020-2021 ($100 \times 70 = 7000$ simulations total per box-plot) done for various values of the α_T parameter ($\alpha_T \in \{0, 0.1, 0.2, 0.5, 0.75, 1\}$). Horizontal lines represent the winter mean temperature of each winter from 1950-1951 to 2020-2021 in ERA5 data. The boxes of the boxplots represent the 25th (q_{25}), median (q_{50}) and 75th (q_{75}) quantiles of the distribution. The upper whisker is $\min\{\max(TN90d), q_{50} + 1.75 \times (q_{75} - q_{25})\}$. The lower whisker corresponds to the lower symmetrical formula.

187 where A_T a normalizing constant, α_T is the importance sampling weight and R_k is the rank (in
 188 ascending order) of the k^{th} analog day among the K analogs.

189 We run the SWG with parameter values $\alpha_T \in \{0, 0.1, 0.2, 0.5, 0.75, 1\}$, starting on each 1st
 190 of December, between 1950 and 2021. If $\alpha_T = 0$, there is no importance sampling and the SWG is
 191 the same as in (Yiou, 2014). Figure 2b shows that for $\alpha_T = 0$, the SWG simulates events covering
 192 the range of winter mean temperatures from 1950-1951 to 2020-2021, apart from winter 1962-1963.
 193 For $\alpha_T = 0.2$, a few outlier simulations reach winter 1963 temperatures. A value of α_T greater than
 194 0.5 allows the simulation of a greater proportion of extreme events. The difference for α_T greater
 195 than 0.5 being less significant, we chose for the following $\alpha_T = 0.5$ as a compromise between the
 196 extreme character of the simulations and their quality.

197 The SWG with importance sampling is obtained by combining the weights on the calendar
 198 and importance sampling. The k^{th} analog day of day t has a probability of:

199
$$\omega_k = A e^{-\alpha_{cal} d_k} e^{-\alpha_T R_k} \quad (3)$$

200 where A is a normalizing constant so that $\sum_{k=1}^K \omega_k = 1$.

201 **2.4 Simulation protocole**

202 We adapted this stochastic weather generator from the one of (Yiou and Jézéquel, 2020),
203 which was designed to simulate summer heat waves, to the version used in this analysis simulating
204 winter cold spells. Consequently, the importance sampling weights favour the coldest analogs instead
205 of the warmest. Furthermore, as the event analysed straddles two years, it is impossible to exclude
206 analogs from the year of the event as it was the case simulating summer heat waves. Thus for winter
207 simulations, analogs of the all length of the observed event are excluded and their weights are put
208 to $w_k = 0$.

209 We refine the original approach of Yiou and Jézéquel (2020) by proposing two different
210 methods simulate SWG trajectories:

- 211 1. Method 1 (*cum data*): At each time step, the simulated day is selected among the $K = 20$
212 analogs and the corresponding day in the observed event (e.g. Dec. 12th 1962 for a simulation
213 initialized on the 1st of December 1962).
- 214 2. Method 2 (*sine data*): At each time step, the selection is made only among the K analogs (the
215 day of the observed event is not considered), and analogs days falling in the observed event
216 are excluded from the selection (e.g. if we initialize a simulation on Dec. 1st 1962 running
217 for $L = 90$ days, all analog day between Dec. 1st 1962 and March 1st 1963 will be excluded).
218 With this method, the simulations use no information from the observed event apart from the
219 initial condition.

220 Method 1 allows the simulation of events that are more like the observed event, while Method 2
221 aims to simulate an ensemble of events possible considering the initial condition and the analogs
222 set only. Therefore, if the SWG is initiated on Dec. 1st 1962 (beginning of the coldest winter), it
223 does not use further information on that record shattering event.

224 The SWG is used to simulate worst-case winter scenario from 1950 to 2021. For each winter
225 from 1950-1951 to 2020-2021, the simulation starts at t_0 — the 1st of December — and run for
226 $L = 90$ days over DJF (December, January and February). $n = 100$ simulations are run by winter
227 year, hence 100×71 events are simulated for each experiment. The α_T and α_{cal} parameters are

228 respectively set to 0.5 and 3.

229 The same process is made using method 1 and method 2. Simulations are also made using
230 the two sets of analogs — the counterfactual and factual periods. Hence the simulated events are
231 events that could have occurred in the analog period used for the simulations. This allows simulating
232 worst case events from the same initial conditions but considering different states of the climate.
233 In other words, we assess whether a record shattering event can be deduced from the information
234 of less intense extremes.

235 In this paper, we focus on winter 1963. We run 1000 simulations starting in December the
236 1st 1962, using as previously, the factual and counterfactual sets of analogs and the two methods.
237 This allows having a wider ensemble of the winter temperature possible starting from the initial
238 conditions of winter 1962-1963.

239 **3 Results**

240 **3.1 Sensitivity to SWG configurations**

241 In this subsection, we simulate cold winters of 90 days starting on a 1st of December of each
242 year from 1950 to 2021. Analogues can be selected in any year from 1950 to 2021. We evaluate the
243 impact of the possibility to sample analogs from the starting year (SWG method 1 vs. method 2)
244 on the winter average temperature. We then evaluate the impact of analog periods on the simulated
245 temperatures.

246 Figure 3 shows the results of simulations from 1951 to 2021 using respectively method 1
247 (Fig. 3a) and method 2 (Fig. 3b) in Section 2, with analogs sampled in 1950-2021. The SWG
248 successfully simulates extremely cold winters, with simulations being respectively 3.9°C (Fig. 3a)
249 and 3.1°C (Fig. 3b) colder overall compared to the ERA5 temperatures time series. 40% of all
250 simulations reach a mean temperature as cold as the 1963 record with method 1, while only 13%
251 of them are as cold using method 2.

252 The variability of the simulations performed with method 1 follows closely the variability of
253 historical winter temperatures due to the possibility of selecting analogs of the observed event with
254 this method. The medians of simulations made with method 1 are highly correlated ($r = 0.88$) to the
255 observed temperatures. With method 2 there is no correlation between the median of simulations

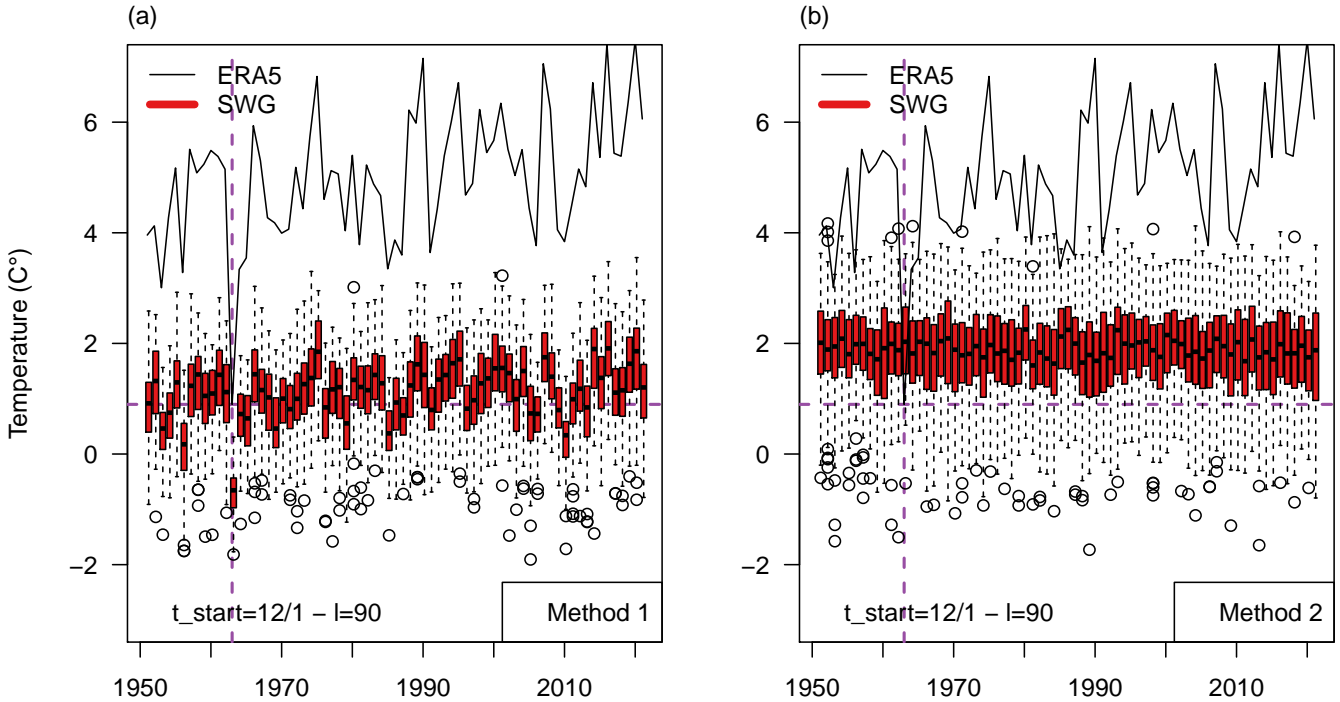


Figure 3: Results of 100 SWG simulations from winter 1950-1951 to winter 2020-2021 with method 1 (a) and method 2 (b). The black continuous line represents the time series of winter mean 2m-temperature over France from ERA5 data. The box plots represent the ensemble variability of the simulations for each year. The boxes of box plots indicate the median (q_{50}), the lower and upper hinges indicate the first (q_{25}) and third (q_{75}) quartiles. The upper whiskers indicate $\min[\max(T), q_{75} + 1.5 \times (q_{75} - q_{25})]$. The lower whisker has a symmetric formulation. The points are the outlying values that are above or below the defined whiskers. The vertical purple dashed line highlights winter 1963 while the vertical purple dashed line shows the mean temperature of the same winter.

256 and the observed temperature, which is the consequence of method 2 not using information from the
 257 observed event apart from the initial conditions. The simulation length of 90 days being higher than
 258 the decorrelation time of atmospheric dynamics, the resulting events should not be highly influenced
 259 by their initial conditions. The standard deviation of the medians of the boxplots obtained with
 260 method 2 is also very low: 0.15°C , compared to the 0.44°C obtained with method 1. This is
 261 coherent with the chaotic internal variability of the climate system, resulting in simulated events
 262 being representative of the climate analogs period used rather than the initial conditions.

263 The mean of boxplots median is also higher by 0.77°C with method 2 compared to method
 264 1, which can be explained by the fact that method 1 allows more days to be picked during the
 265 importance sampling process so that the coldest days can be selected during the simulations by
 266 construction, while some analogs days are excluded when using method 2.

267 Simulating winter with Method 2 using analogs either in the factual (1972-2021) or counter-

268 factual (1950-1999) periods gives an overview of the range of the most extreme winter temperatures
269 possible in those two climate periods. With method 2, winter simulations in the factual period are
270 overall warmer of 0.73°C compared to the counterfactual period. This difference has the same order
271 of magnitude as the observed warming of 0.52°C between winter mean temperatures in the factual
272 and counterfactual periods. This is also consistent with a current warming rate of 0.36°C per decade
273 in metropolitan France, as estimated by Ribes et al. (2022), which corresponds to a warming of
274 approximately 0.72°C between the factual and counterfactual periods. For 1963, method 2 excludes
275 the use of any analog day in winter 1962-1963 for simulating the events. The only information of
276 winter 1962-1963 used is the initial condition of the 1st December 1963. By excluding all informa-
277 tion from this exceptional event of the 1950-1999 simulations, the difference between simulations
278 using 1972-2021 analogs compared to 1950-1999 analogs is of only 0.16°C , which is lower than for
279 other years.

280 **3.2 Focus on winter 1963**

281 In this subsection, we simulate winter 1962-1963, starting on Dec. 1st 1962, and consider
282 circulation analogs in the counterfactual and factual periods. Here, 1000 simulations are done for
283 that winter. Figure 4a shows the focus on 1963 simulations using methods 1 and 2 and the factual
284 and counterfactual analogs periods. As seen in Section 2, the simulations are overall colder using
285 method 1 than method 2. This is also the case for 1963; as displayed in Figure 4a for both the
286 factual and counterfactual period. All events simulated with method 1 reach a mean temperature
287 over DJF colder than the value reached in 1963 whether using 1950-1999 or 1972-2021 analogs.

288 The probability of reaching winter 1963 temperatures is lower with method 2. The first
289 quantile of simulations does not reach 1963 mean values both in the factual and counterfactual
290 periods. 1963 was already a very rare event in the 1950-1999 climate but remains reachable using
291 only 1971-2021 analogs, in a climate with more global warming.

292 Figure 4b displays the time series associated with 1963 simulations using method 2. The
293 temperatures of winter 1962-1963 are below the seasonal cycle for most of the season. The tem-
294 peratures of simulated events for both the factual and counterfactual periods are also overall well
295 below the seasonal mean for the all length of the event. The median fluctuates around 2°C while
296 the 5_{th} percentile of all simulation reaches -5°C during most of the winter. The 95_{th} percentile
297 stays under 2°C above the seasonal average while the 5th percentile reaches -4°C during most of

298 the event, which corresponds to the coldest daily mean temperatures observed in 1963. Overall the
 299 range of daily winter temperatures as simulated for extreme winter temperatures matches the range
 300 of daily mean temperatures observed in 1962-1963 extreme winter event in both the factual and
 301 counterfactual periods. Hence a winter like the one of 1962-1963, even if of very low probability,
 302 could still be possible under a warmer climate of the 21st century.

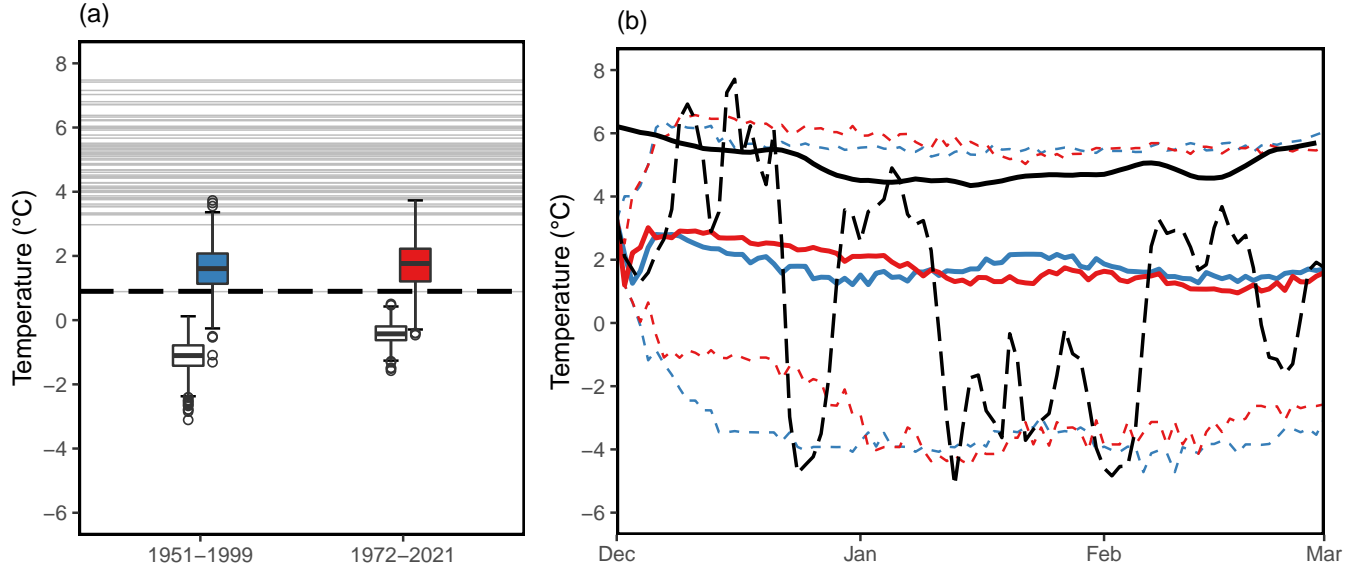


Figure 4: (a) Temperature distribution of 1000 SWG simulations of winter 1962-1963 with analogs from 1950-1999 (left) or 1972-2021 (right) in ERA5 data using method 1 (white filled boxplots) and method 2 (color filled boxplots). Horizontal lines represent the winter mean temperature of each winter from 1950-1951 to 2020-2021 in ERA5 data. The dashed black line is the value that was observed in 1962-1963. (b) Time series of 7-day running mean of daily mean temperatures for winter 1962-1963 (dashed black line), SWG median (plain line), q05 and q95 (dashed lines) temperatures of the thousand 1962-1963 simulations with Method 2 using 1950-1999 analogs (blue lines) and 1972-2021 analogs (red lines).

3.3 Atmospheric dynamics during winter 1963

A strong and persisting anticyclonic anomaly prevailed over Iceland. It was associated with a negative Z500 anomaly over continental Europe, the Azores and the Glacial Arctic Ocean, leading to a weakening of the westerlies and advection of cold air from the Arctic (Fig. 5a).

Here, we compute the composites of Z500 and Z500 anomalies over a region that is larger than the region for which the analogs are computed.

The Z500 composite over DJF does not correspond directly to a North Atlantic weather pattern, as for instance obtained by Cattiaux et al. (2010). The low over Europe is located more to the East than for an NAO- weather pattern, while the positive Z500 anomaly over Iceland is located more to the north than it would be in an Atlantic ridge weather regime. The respectively

313 positive and negative Z500 anomalies over Iceland and the Azores are however characteristic of a
 314 negative NAO index which is often, even if not systematically, an indicator of colder than usual
 315 winter temperature over Europe (Hirschi and Sinha, 2007).

316 Z500 anomalies of SWG simulations for winter 1963 are smoother than the ERA5 field for
 317 the same winter. This can be explained by the fact that the map is averaged over 100 (10% of
 318 1000 simulations) different simulations and that simulations are less auto-correlated than observed
 319 events would be, thus having more spatial variability. Hence, we compute the Z500 and Z500
 320 anomaly composites of SWG simulations for the 10% coldest members of the ensemble starting on
 321 Dec. 1st 1962. For comparison purposes with winter 1963, this selection is reasonable because 75%
 322 of simulations are warmer than this record event (Fig. 4a), and we want to focus on the coldest
 323 members of the ensemble. We find that the pattern of a strong negative anomaly over Western
 324 Europe and a positive anomaly over Iceland is still reflected in the 10% coldest events simulated
 325 with the SWG in both the counterfactual (Fig. 5b) and factual (Fig. 5c) simulations. The intensity
 326 and position of the Z500 low over the Barents sea and the high over western Russia seen in ERA5
 327 seem to have a lower contribution to the intensity of the event as they are weaker and less marked
 328 in the SWG simulated events.

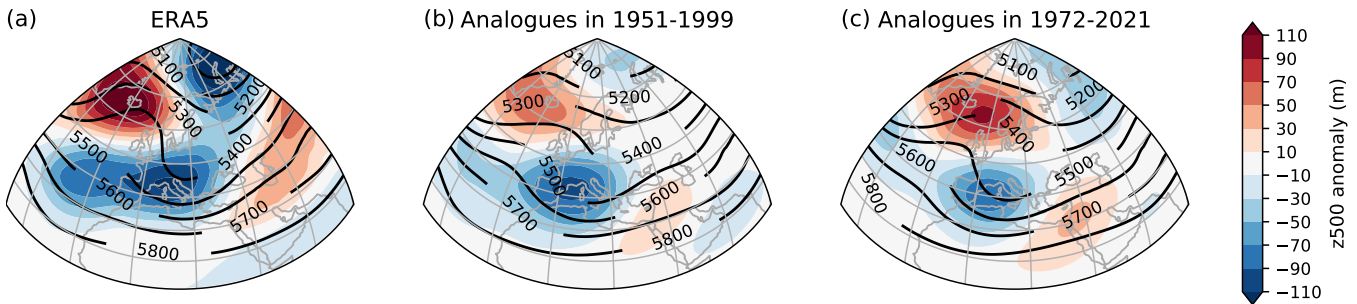


Figure 5: Absolute values (contours) and anomalies with respect to 1950-2021 (shaded areas) of 500-hPa geopotential height (Z500) average over DJF for winter 1963 as observed in ERA5 (a) and simulated by the SWG with counterfactual (b) and factual (c) analogs using method 2 (sine data). For the simulations, the composite maps are computed from the 10% coldest simulations among the 1000 (i.e. 100 simulations per map).

329 4 Discussion and conclusion

330 This paper presents how an analog stochastic weather generator can be used to simulate
 331 ensembles of extreme cold winters in continental France. We adapted the method developed by
 332 Yiou and Jézéquel (2020) (to simulate extreme heat waves) to the simulation of extreme cold

333 events. The paper displays a proof of concept using ERA5 data for the simulation of extreme
334 winter temperatures in France between 1950 and 2021.

335 The SWG for the simulation of extreme cold spells inherits some of the technical caveats
336 already pointed out by Yiou and Jézéquel (2020) for the simulation of extreme heat waves. This
337 SWG method is limited by the length of the data set used as input, so that it may not sample
338 completely the atmospheric dynamics of the climate system. The average of resampled analogs is
339 however bounded to a lesser extent and can reach values far more extreme than the most extreme
340 ones in the input data set. The SWG allows simulation of extreme events outside the observed
341 range but is still limited by the length of available data.

342 The length of the factual and counterfactual periods considered was a compromise between
343 the length of available data (70 years), the non stationarity of temperatures and the overlapping of
344 the two periods. We needed periods of sufficient length to sample correctly the climate considered.
345 But to have significant differences between the factual and counterfactual periods it was better
346 that they would overlap as little as possible. The non stationarity of climate also means that
347 the longer the periods, the less homogeneous they are in terms of level of warming. 50-year long
348 periods yield good results in terms of both extremeness (the data set is large enough to simulated
349 very rare events) and significant enough difference between the factual and counterfactual periods.
350 Moreover we verified that the analog days are evenly distributed over the two climate periods and
351 evenly picked during the simulation process. Therefore we consider that the events simulated are
352 representative of the entire analogs period used in the SWG.

353 This method does not allow to disentangle anthropogenic warming from others forcings and
354 natural multi-decadal variability of the climate system. But it gives an estimation of the worst-case
355 winter temperatures scenario for a given climate as sampled is the input. Another caveat is that
356 the method is mainly based on the use of flow analogs to assess temperatures. It focuses on the link
357 between atmospheric circulation and temperatures and does not take into account other drivers and
358 feed-backs. For instance, snow cover is not considered in the simulations even though it can have a
359 significant impact on extreme winter temperatures (Orsolini et al., 2013).

360 We showed that winter as cold as the record event of 1963 or even colder could still occur
361 in the current climate, at a higher level of warming. This does not mean than such an event will
362 happen in the future but it remains possible at the considered level of warming and is relevant

363 from an adaptation point of view. A winter as cold as 1963 would indeed have major impacts
364 on society, especially on the energy system (Añel et al., 2017). For instance, Doss-Gollin et al.
365 (2021) showed that the February 2021 Texas cold snap, which resulted in major failures of the
366 energy system causing energy, food and water shortages, was actually not unprecedented both in
367 terms of temperature anomalies and resulting heating demand per capita. The lack of preparedness
368 and greater exposure of the energy system due to increasing population and electrification led to
369 disproportionate impacts. In France, the electricity transmission system operator RTE (Réseau de
370 Transport d'Électricité) estimates the sensitivity of electricity consumption to temperature to be
371 2400 MW/°C in winter (RTE, 2021). Hence, it might be desirable that energy systems and logistics
372 are scaled for worst case winter scenario in the current or future climate conditions and exposure
373 as the ones simulated in this study.

374 The possible occurrence of unprecedented cold winter temperatures in France as simulated
375 in this paper is not inconsistent with the already observed decrease in cold spells intensity in the
376 northern mid-latitudes as exposed by Van Oldenborgh et al. (2019). We focus here on low-likelihood
377 long-lasting events, with a return period of over 10^3 years. This is not representative of cold waves
378 defined as the exceeding of a threshold over a few days, which can be a yearly event.

379 The absence of significant changes in the atmospheric circulation leading to the extreme
380 winters simulated is in line with the *typicality* of large and persistent temperature anomalies as
381 shown using large deviation theory (Gálfi and Lucarini (2020); Gálfi et al. (2021)). The same
382 atmospheric conditions usually lead to the most extreme events. However these results are valid in
383 a stationary system and obtained using steady state model simulations. Climate change can lead to
384 important shifts in atmospheric dynamics that could affect the frequency and intensity of extreme
385 events, as well as the dynamics leading to them. The present paper shows no significant shift in the
386 atmospheric circulation of record-breaking winters between the factual and counterfactual periods,
387 which have a difference 0.72°C in terms of level of warming. However these results cannot be
388 extended to a higher shift in global warming level. Simulations of extreme cold spells using of the
389 Coupled Model Intercomparison Project phase 6 (CMIP6) simulations (Eyring et al., 2016) would
390 therefore be an extension of this study in order to further explore the evolution of extreme winter
391 temperatures in the mid-latitudes in the future — according to different emissions pathways (Riahi
392 et al., 2017) — and the associated atmospheric trajectories.

393 In this paper, we focused on cold winters (90 days: TN90d) in France. The method can be
394 adapted to simulate cold events of different duration, or in other regions. The worst cold spells
395 recorded in France were February 1956 — the coldest month of the 20st century (Andrews, 1956;
396 Dizerens et al., 2017) — and January 1985 (Météo France, 2022a,b). These events caused major
397 disruptions and had a wide health impact (Huynen et al., 2001). The energy sector has been sensitive
398 to 15-day events. The cold spell of 3rd – 17th January 1985 is used as the event of reference by
399 the French electrical network company. A similar event triggered an unprecedented impulse of
400 solidarity, following Abbé Pierre’s call in France for the help of the homeless during winter 1954.

401 Winter 1963 was the coldest winter recorded in France and a record-shattering event. Using
402 an analog stochastic weather generator with importance sampling for the simulation of an extremely
403 cold winter, we show that winter 1963 temperatures were already exceptional in the lower level of
404 warming in which it occurred. Estimations of the possibility of such an extreme event occurring
405 in the recent climate show that it is still possible to have a winter as cold, even if would remain a
406 highly exceptional event. This paper hence provides a *storyline* for extremely cold winters in France
407 (Sillmann et al., 2021).

408 **Declaration of competing interest**

409 The authors declare that they have no known competing financial interests or personal
410 relationships that could have appeared to influence the work reported in this paper.

411 **Acknowledgments**

412 The authors acknowledge the support of the grant ANR-20-CE01-0008-01 (SAMPRACE:
413 PY, CC). This work also received support from the European Union’s Horizon 2020 research and
414 innovation programme under grant agreement No. 101003469 (XAIDA: PY).

415 **References**

416 P. Ailliot, D. Allard, V. Monbet, and P. Naveau. Stochastic weather generators: an
417 overview of weather type models. *Journal de la Société Française de Statistique*,
418 2015. URL [https://www.researchgate.net/publication/272504645_Stochastic_weather_](https://www.researchgate.net/publication/272504645_Stochastic_weather_generators_An_overview_of_weather_type_models)
419 [generators_An_overview_of_weather_type_models](https://www.researchgate.net/publication/272504645_Stochastic_weather_generators_An_overview_of_weather_type_models). Pages: 101-113 Volume: 156 Issue: 1
420 ISSN: 1962-5197.

421 J. F. Andrews. THE WEATHER AND CIRCULATION OF FEBRUARY 1956: Including a Dis-

422 cussion of Persistent Blocking and Severe Weather in Europe. *Monthly Weather Review*, 84(2):66–
423 74, Feb. 1956. ISSN 1520-0493, 0027-0644. doi: 10.1175/1520-0493(1956)084(0066:TWACOF)2.
424 0.CO;2. URL [https://journals.ametsoc.org/view/journals/mwre/84/2/1520-0493_1956_](https://journals.ametsoc.org/view/journals/mwre/84/2/1520-0493_1956_084_0066_twacof_2_0_co_2.xml)
425 [084_0066_twacof_2_0_co_2.xml](https://journals.ametsoc.org/view/journals/mwre/84/2/1520-0493_1956_084_0066_twacof_2_0_co_2.xml). Publisher: American Meteorological Society Section: Monthly
426 Weather Review.

427 J. A. Añel, M. Fernández-González, X. Labandeira, X. López-Otero, and L. De la Torre. Impact
428 of Cold Waves and Heat Waves on the Energy Production Sector. *Atmosphere*, 8(11):209, Nov.
429 2017. ISSN 2073-4433. doi: 10.3390/atmos8110209. URL [https://www.mdpi.com/2073-4433/](https://www.mdpi.com/2073-4433/8/11/209)
430 [8/11/209](https://www.mdpi.com/2073-4433/8/11/209). Number: 11 Publisher: Multidisciplinary Digital Publishing Institute.

431 M. Bessec and J. Fouquau. The non-linear link between electricity consumption and temperature
432 in Europe: A threshold panel approach. *Energy Economics*, 30(5):2705–2721, Sept. 2008. ISSN
433 0140-9883. doi: 10.1016/j.eneco.2008.02.003. URL [https://www.sciencedirect.com/science/](https://www.sciencedirect.com/science/article/pii/S0140988308000418)
434 [article/pii/S0140988308000418](https://www.sciencedirect.com/science/article/pii/S0140988308000418).

435 R. Blackport and J. A. Screen. Insignificant effect of Arctic amplification on the amplitude of
436 midlatitude atmospheric waves. *Science Advances*, 6(8):eaay2880, Feb. 2020. doi: 10.1126/
437 sciadv.aay2880. URL <https://www.science.org/doi/10.1126/sciadv.aay2880>. Publisher:
438 American Association for the Advancement of Science.

439 J. Cattiaux, R. Vautard, C. Cassou, P. Yiou, V. Masson-Delmotte, and F. Codron. Winter 2010 in
440 Europe: A cold extreme in a warming climate. *Geophysical Research Letters*, 37(20):20704, Oct.
441 2010. ISSN 00948276. doi: 10.1029/2010GL044613. URL [https://onlinelibrary.wiley.com/](https://onlinelibrary.wiley.com/doi/full/10.1029/2010GL044613)
442 [doi/full/10.1029/2010GL044613](https://onlinelibrary.wiley.com/doi/full/10.1029/2010GL044613). Publisher: John Wiley & Sons, Ltd.

443 S. E. Chang, T. L. McDaniels, J. Mikawoz, and K. Peterson. Infrastructure failure interdependencies
444 in extreme events: power outage consequences in the 1998 Ice Storm. *Natural Hazards*, 41(2):
445 337–358, May 2007. ISSN 1573-0840. doi: 10.1007/s11069-006-9039-4. URL [https://doi.org/](https://doi.org/10.1007/s11069-006-9039-4)
446 [10.1007/s11069-006-9039-4](https://doi.org/10.1007/s11069-006-9039-4).

447 J. Cohen, J. A. Screen, J. C. Furtado, M. Barlow, D. Whittleston, D. Coumou, J. Francis,
448 K. Dethloff, D. Entekhabi, J. Overland, and J. Jones. Recent Arctic amplification and ex-
449 treme mid-latitude weather. *Nature Geoscience*, 7(9):627–637, Aug. 2014. ISSN 17520908. doi:

450 10.1038/ngeo2234. URL <https://www.nature.com/articles/ngeo2234>. Publisher: Nature
451 Publishing Group.

452 J. Cohen, X. Zhang, J. Francis, T. Jung, R. Kwok, J. Overland, T. J. Ballinger, U. S. Bhatt, H. W.
453 Chen, D. Coumou, S. Feldstein, H. Gu, D. Handorf, G. Henderson, M. Ionita, M. Kretschmer,
454 F. Laliberte, S. Lee, H. W. Linderholm, W. Maslowski, Y. Peings, K. Pfeiffer, I. Rigor, T. Semm-
455 ler, J. Stroeve, P. C. Taylor, S. Vavrus, T. Vihma, S. Wang, M. Wendisch, Y. Wu, and J. Yoon.
456 Divergent consensuses on Arctic amplification influence on midlatitude severe winter weather. *Nature*
457 *Climate Change*, 10(1):20–29, Jan. 2020. ISSN 1758-6798. doi: 10.1038/s41558-019-0662-y.
458 URL <https://www.nature.com/articles/s41558-019-0662-y>. Number: 1 Publisher: Nature
459 Publishing Group.

460 S. Corti, F. Molteni, and T. Palmer. Signature of recent climate change in frequencies of natural
461 atmospheric circulation regimes. *Nature*, 398(6730):799–802, 1999.

462 A. Dawson, T. N. Palmer, and S. Corti. Simulating regime structures in weather and cli-
463 mate prediction models. *Geophysical Research Letters*, 39(21), 2012. doi: [https://doi.org/10.](https://doi.org/10.1029/2012GL053284)
464 [1029/2012GL053284](https://doi.org/10.1029/2012GL053284). URL [https://agupubs.onlinelibrary.wiley.com/doi/abs/10.1029/](https://agupubs.onlinelibrary.wiley.com/doi/abs/10.1029/2012GL053284)
465 [2012GL053284](https://agupubs.onlinelibrary.wiley.com/doi/abs/10.1029/2012GL053284).

466 C. Dizerens, S. Lenggenhager, M. Schwander, A. Buck, and S. Foffa. The 1956 Cold Wave in Western
467 Europe. *Geographica Bernensia*, 2017. URL <https://doi.org/10.4480/GB2017.G92.09>.

468 J. Doss-Gollin, D. J. Farnham, U. Lall, and V. Modi. How unprecedented was the February 2021
469 Texas cold snap? *Environmental Research Letters*, 16(6):064056, June 2021. ISSN 1748-9326.
470 doi: 10.1088/1748-9326/ac0278. URL <https://dx.doi.org/10.1088/1748-9326/ac0278>. Pub-
471 lisher: IOP Publishing.

472 V. Eyring, S. Bony, G. A. Meehl, C. A. Senior, B. Stevens, R. J. Stouffer, and K. E. Taylor.
473 Overview of the Coupled Model Intercomparison Project Phase 6 (CMIP6) experimental design
474 and organization. *Geoscientific Model Development*, 9(5):1937–1958, May 2016. ISSN 19919603.
475 doi: 10.5194/GMD-9-1937-2016. Publisher: Copernicus GmbH.

476 E. M. Fischer, S. Sippel, and R. Knutti. Increasing probability of record-shattering climate ex-
477 tremes. *Nature Climate Change*, 11(8):689–695, July 2021. ISSN 17586798. doi: 10.1038/

478 s41558-021-01092-9. URL <https://www.nature.com/articles/s41558-021-01092-9>. Pub-
479 lisher: Nature Publishing Group.

480 J. A. Francis. Why Are Arctic Linkages to Extreme Weather Still up in the Air? *Bulletin of the*
481 *American Meteorological Society*, 98(12):2551–2557, Dec. 2017. ISSN 0003-0007, 1520-0477. doi:
482 10.1175/BAMS-D-17-0006.1. URL [https://journals.ametsoc.org/view/journals/bams/98/](https://journals.ametsoc.org/view/journals/bams/98/12/bams-d-17-0006.1.xml)
483 [12/bams-d-17-0006.1.xml](https://journals.ametsoc.org/view/journals/bams/98/12/bams-d-17-0006.1.xml). Publisher: American Meteorological Society Section: Bulletin of the
484 American Meteorological Society.

485 J. A. Francis and S. J. Vavrus. Evidence linking Arctic amplification to extreme weather in mid-
486 latitudes. *Geophysical Research Letters*, 39(6), Mar. 2012. ISSN 1944-8007. doi: 10.1029/
487 2012GL051000. URL <https://onlinelibrary.wiley.com/doi/full/10.1029/2012GL051000>.
488 Publisher: John Wiley & Sons, Ltd.

489 J. A. Francis, N. Skific, and S. J. Vavrus. North American Weather Regimes
490 Are Becoming More Persistent: Is Arctic Amplification a Factor? *Geophys-*
491 *ical Research Letters*, 45(20):11,414–11,422, 2018. ISSN 1944-8007. doi: 10.1029/
492 2018GL080252. URL <https://onlinelibrary.wiley.com/doi/abs/10.1029/2018GL080252>.
493 eprint: <https://onlinelibrary.wiley.com/doi/pdf/10.1029/2018GL080252>.

494 V. M. Galfi and V. Lucarini. Fingerprinting Heatwaves and Cold Spells and Assessing Their Re-
495 sponse to Climate Change using Large Deviation Theory. *Physical Review Letters*, 127(5), Oct.
496 2020. doi: 10.1103/PhysRevLett.127.058701. URL <http://arxiv.org/abs/2010.08272>. arXiv:
497 2010.08272v1 Publisher: American Physical Society.

498 A. Gasparrini, Y. Guo, M. Hashizume, E. Lavigne, A. Zanobetti, J. Schwartz, A. Tobias, S. Tong,
499 J. Rocklöv, B. Forsberg, M. Leone, M. D. Sario, M. L. Bell, Y.-L. L. Guo, C.-f. Wu, H. Kan, S.-M.
500 Yi, M. d. S. Z. S. Coelho, P. H. N. Saldiva, Y. Honda, H. Kim, and B. Armstrong. Mortality
501 risk attributable to high and low ambient temperature: a multicountry observational study. *The*
502 *Lancet*, 386(9991):369–375, July 2015. ISSN 0140-6736, 1474-547X. doi: 10.1016/S0140-6736(14)
503 62114-0. URL [https://www.thelancet.com/journals/lancet/article/PIIS0140-6736\(14\)](https://www.thelancet.com/journals/lancet/article/PIIS0140-6736(14)62114-0/fulltext)
504 [62114-0/fulltext](https://www.thelancet.com/journals/lancet/article/PIIS0140-6736(14)62114-0/fulltext). Publisher: Elsevier.

505 R. J. Greatbatch. The North Atlantic Oscillation. *Stochastic Environmental Research and Risk*

506 *Assessment*, 14(4):213–242, Sept. 2000. ISSN 1436-3259. doi: 10.1007/s004770000047. URL
507 <https://doi.org/10.1007/s004770000047>.

508 R. J. Greatbatch, G. Gollan, T. Jung, and T. Kunz. Tropical origin of the severe European winter
509 of 1962/1963. *Quarterly Journal of the Royal Meteorological Society*, 141(686):153–165, 2015.
510 ISSN 1477-870X. doi: 10.1002/qj.2346. URL [https://onlinelibrary.wiley.com/doi/abs/
511 10.1002/qj.2346](https://onlinelibrary.wiley.com/doi/abs/10.1002/qj.2346). eprint: <https://onlinelibrary.wiley.com/doi/pdf/10.1002/qj.2346>.

512 V. M. Gálfi, V. Lucarini, F. Ragone, and J. Wouters. Applications of large deviation theory in
513 geophysical fluid dynamics and climate science. *La Rivista del Nuovo Cimento*, 44(6):291–363,
514 June 2021. ISSN 1826-9850. doi: 10.1007/s40766-021-00020-z. URL [https://doi.org/10.
515 1007/s40766-021-00020-z](https://doi.org/10.1007/s40766-021-00020-z).

516 N. Hempelmann, C. Ehbrecht, C. Alvarez-Castro, P. Brockmann, W. Falk, J. Hoffmann, S. Kinder-
517 mann, B. Koziol, C. Nangini, S. Radanovics, R. Vautard, and P. Yiou. Web processing service
518 for climate impact and extreme weather event analyses. Flyingpigeon (Version 1.0). *Computers
519 & Geosciences*, 110:65–72, Jan. 2018. ISSN 0098-3004. doi: 10.1016/j.cageo.2017.10.004. URL
520 <https://www.sciencedirect.com/science/article/pii/S0098300416302801>.

521 H. Hersbach, B. Bell, P. Berrisford, S. Hirahara, A. Horányi, J. Muñoz-Sabater, J. Nicolas,
522 C. Peubey, R. Radu, D. Schepers, A. Simmons, C. Soci, S. Abdalla, X. Abellan, G. Balsamo,
523 P. Bechtold, G. Biavati, J. Bidlot, M. Bonavita, G. De Chiara, P. Dahlgren, D. Dee, M. Dia-
524 mantakis, R. Dragani, J. Flemming, R. Forbes, M. Fuentes, A. Geer, L. Haimberger, S. Healy,
525 R. J. Hogan, E. Hólm, M. Janisková, S. Keeley, P. Laloyaux, P. Lopez, C. Lupu, G. Radnoti,
526 P. de Rosnay, I. Rozum, F. Vamborg, S. Villaume, and J. N. Thépaut. The ERA5 global reanaly-
527 sis. *Quarterly Journal of the Royal Meteorological Society*, 146(730):1999–2049, July 2020. ISSN
528 1477870X. doi: 10.1002/QJ.3803. Publisher: John Wiley and Sons Ltd.

529 J. J.-M. Hirschi and B. Sinha. Negative NAO and cold Eurasian winters: how exceptional
530 was the winter of 1962/1963? *Weather*, 62(2):43–48, 2007. ISSN 1477-8696. doi: 10.
531 1002/wea.34. URL <https://onlinelibrary.wiley.com/doi/abs/10.1002/wea.34>. eprint:
532 <https://onlinelibrary.wiley.com/doi/pdf/10.1002/wea.34>.

533 D. E. Horton, N. C. Johnson, D. Singh, D. L. Swain, B. Rajaratnam, and N. S. Diffenbaugh. Con-
534 tribution of changes in atmospheric circulation patterns to extreme temperature trends. *Nature*,

522(7557):465–469, June 2015. ISSN 0028-0836, 1476-4687. doi: 10.1038/nature14550. URL
536 <http://www.nature.com/articles/nature14550>.

537 J. W. Hurrell, Y. Kushnir, G. Ottersen, and M. Visbeck. An Overview of the North At-
538 lantic Oscillation. In *The North Atlantic Oscillation: Climatic Significance and Environmen-
539 tal Impact*, pages 1–35. American Geophysical Union (AGU), 2003. ISBN 978-1-118-66903-7.
540 doi: 10.1029/134GM01. URL <https://onlinelibrary.wiley.com/doi/abs/10.1029/134GM01>.
541 eprint: <https://onlinelibrary.wiley.com/doi/pdf/10.1029/134GM01>.

542 M. M. Huynen, P. Martens, D. Schram, M. P. Weijenberg, and A. E. Kunst. The impact of
543 heat waves and cold spells on mortality rates in the Dutch population. *Environmental Health
544 Perspectives*, 109(5):463–470, May 2001. doi: 10.1289/ehp.01109463. URL [https://ehp.niehs.
545 nih.gov/doi/10.1289/ehp.01109463](https://ehp.niehs.nih.gov/doi/10.1289/ehp.01109463). Publisher: Environmental Health Perspectives.

546 A. Jézéquel, P. Yiou, and S. Radanovics. Role of circulation in European heatwaves using
547 flow analogues. *Climate Dynamics*, 50(3-4):1145–1159, 2018. ISSN 14320894. doi: 10.1007/
548 s00382-017-3667-0. URL <https://hal.archives-ouvertes.fr/hal-01373903v2>. Publisher:
549 Springer Verlag.

550 M. Krouma, P. Yiou, C. Déandreis, and S. Thao. Assessment of stochastic weather forecast of
551 precipitation near European cities, based on analogs of circulation. *Geoscientific Model Devel-
552 opment*, 15(12):4941–4958, June 2022. ISSN 1991-959X. doi: 10.5194/gmd-15-4941-2022. URL
553 <https://gmd.copernicus.org/articles/15/4941/2022/>. Publisher: Copernicus GmbH.

554 Met office. Severe Winters. URL [https://www.metoffice.gov.uk/weather/learn-about/
555 weather/case-studies/severe-winters](https://www.metoffice.gov.uk/weather/learn-about/weather/case-studies/severe-winters).

556 Météo France. Hivers : où sont passées les vagues de froid ?, Feb.
557 2022a. URL [https://meteofrance.com/actualites-et-dossiers/magazine/
558 hivers-ou-sont-passees-les-vagues-de-froid](https://meteofrance.com/actualites-et-dossiers/magazine/hivers-ou-sont-passees-les-vagues-de-froid).

559 Météo France. Retour sur la vague de froid de janvier 1987, Jan.
560 2022b. URL [https://meteofrance.com/actualites-et-dossiers/magazine/
561 retour-sur-la-vague-de-froid-de-janvier-1987](https://meteofrance.com/actualites-et-dossiers/magazine/retour-sur-la-vague-de-froid-de-janvier-1987).

- 562 J. F. O’connor. THE WEATHER AND CIRCULATION OF JANUARY 1963: One of the Most
563 Severe Months on Record in the United States and Europe. *Monthly Weather Review*, 91(4):209–
564 218, Apr. 1963. ISSN 1520-0493, 0027-0644. doi: 10.1175/1520-0493(1963)091<0209:TWAC0J>2.
565 3.CO;2. URL [https://journals.ametsoc.org/view/journals/mwre/91/4/1520-0493_1963_](https://journals.ametsoc.org/view/journals/mwre/91/4/1520-0493_1963_091_0209_twacoj_2_3_co_2.xml)
566 [091_0209_twacoj_2_3_co_2.xml](https://journals.ametsoc.org/view/journals/mwre/91/4/1520-0493_1963_091_0209_twacoj_2_3_co_2.xml). Publisher: American Meteorological Society Section: Monthly
567 Weather Review.
- 568 Y. J. Orsolini, R. Senan, G. Balsamo, F. J. Doblas-Reyes, F. Vitart, A. Weisheimer, A. Carrasco,
569 and R. E. Benestad. Impact of snow initialization on sub-seasonal forecasts. *Climate Dynamics*,
570 41(7):1969–1982, Oct. 2013. ISSN 1432-0894. doi: 10.1007/s00382-013-1782-0. URL [https:](https://doi.org/10.1007/s00382-013-1782-0)
571 [//doi.org/10.1007/s00382-013-1782-0](https://doi.org/10.1007/s00382-013-1782-0).
- 572 J. E. Overland, K. Dethloff, J. A. Francis, R. J. Hall, E. Hanna, S.-J. Kim, J. A. Screen, T. G. Shep-
573 herd, and T. Vihma. Nonlinear response of mid-latitude weather to the changing Arctic. *Nature*
574 *Climate Change*, 6(11):992–999, Nov. 2016. ISSN 1758-6798. doi: 10.1038/nclimate3121. URL
575 <https://www.nature.com/articles/nclimate3121>. Number: 11 Publisher: Nature Publishing
576 Group.
- 577 P. Platzner, P. Yiou, P. Naveau, P. Tandeo, J.-F. Filipot, P. Ailliot, and Y. Zhen. Using Local
578 Dynamics to Explain Analog Forecasting of Chaotic Systems. *Journal of the Atmospheric Sci-*
579 *ences*, 78(7):2117–2133, July 2021. ISSN 0022-4928, 1520-0469. doi: 10.1175/JAS-D-20-0204.
580 1. URL <https://journals.ametsoc.org/view/journals/atsc/78/7/JAS-D-20-0204.1.xml>.
581 Publisher: American Meteorological Society Section: Journal of the Atmospheric Sciences.
- 582 F. Ragone and F. Bouchet. Rare Event Algorithm Study of Extreme Warm Summers and Heat-
583 waves Over Europe. *Geophysical Research Letters*, 48(12):e2020GL091197, 2021. ISSN 1944-
584 8007. doi: 10.1029/2020GL091197. URL [https://onlinelibrary.wiley.com/doi/abs/10.](https://onlinelibrary.wiley.com/doi/abs/10.1029/2020GL091197)
585 [1029/2020GL091197](https://onlinelibrary.wiley.com/doi/abs/10.1029/2020GL091197). eprint: <https://onlinelibrary.wiley.com/doi/pdf/10.1029/2020GL091197>.
- 586 K. Riahi, D. P. van Vuuren, E. Kriegler, J. Edmonds, B. C. O’Neill, S. Fujimori, N. Bauer, K. Calvin,
587 R. Dellink, O. Fricko, W. Lutz, A. Popp, J. C. Cuaresma, S. KC, M. Leimbach, L. Jiang, T. Kram,
588 S. Rao, J. Emmerling, K. Ebi, T. Hasegawa, P. Havlik, F. Humpenöder, L. A. Da Silva, S. Smith,
589 E. Stehfest, V. Bosetti, J. Eom, D. Gernaat, T. Masui, J. Rogelj, J. Strefler, L. Drouet, V. Krey,
590 G. Luderer, M. Harmsen, K. Takahashi, L. Baumstark, J. C. Doelman, M. Kainuma, Z. Klimont,
591 G. Marangoni, H. Lotze-Campen, M. Obersteiner, A. Tabeau, and M. Tavoni. The Shared

592 Socioeconomic Pathways and their energy, land use, and greenhouse gas emissions implications:
593 An overview. *Global Environmental Change*, 42:153–168, Jan. 2017. ISSN 09593780. doi: 10.
594 1016/J.GLOENVCHA.2016.05.009. Publisher: Elsevier Ltd.

595 A. Ribes, J. Boé, S. Qasmi, B. Dubuisson, H. Douville, and L. Terray. An updated assessment of
596 past and future warming over France based on a regional observational constraint. *Earth System*
597 *Dynamics*, 13(4):1397–1415, Oct. 2022. ISSN 2190-4979. doi: 10.5194/esd-13-1397-2022. URL
598 <https://esd.copernicus.org/articles/13/1397/2022/>. Publisher: Copernicus GmbH.

599 S. M. Robeson, C. J. Willmott, and P. D. Jones. Trends in hemispheric warm and cold anoma-
600 lies. *Geophysical Research Letters*, 41(24):9065–9071, 2014. ISSN 1944-8007. doi: 10.1002/
601 2014GL062323. URL <https://onlinelibrary.wiley.com/doi/abs/10.1002/2014GL062323>.
602 _eprint: <https://onlinelibrary.wiley.com/doi/pdf/10.1002/2014GL062323>.

603 RTE. Bilan électrique 2020. Technical report, RTE, Mar. 2021. URL [https://](https://bilan-electrique-2020.rte-france.com/#)
604 bilan-electrique-2020.rte-france.com/#.

605 S. Seneviratne, X. Zhang, M. Adnan, W. Badi, C. Dereczynski, A. Di Luca, S. Ghosh, I. Iskandar,
606 J. Kossin, S. Lewis, F. Otto, I. Pinto, M. Satoh, S. Vicente-Serrano, M. Wehner, and B. Zhou.
607 Weather and Climate Extreme Events in a Changing Climate. In V. Masson-Delmotte, P. Zhai,
608 A. Pirani, S. Connors, C. Péan, S. Berger, N. Caud, Y. Chen, L. Goldfarb, M. Gomis, M. Huang,
609 K. Leitzell, E. Lonnoy, J. Matthews, T. Maycock, T. Waterfield, O. Yelekçi, R. Yu, and B. Zhou,
610 editors, *Climate Change 2021: The Physical Science Basis. Contribution of Working Group I to*
611 *the Sixth Assessment Report of the Intergovernmental Panel on Climate Change*, pages 1513–
612 1766. Cambridge University Press, Cambridge, United Kingdom and New York, NY, USA, 2021.
613 doi: 10.1017/9781009157896.013.

614 A. Shabbar, J. Huang, and K. Higuchi. The relationship between the wintertime North Atlantic
615 oscillation and blocking episodes in the North Atlantic. *International Journal of Climatology*, 21
616 (3):355–369, Mar. 2001. ISSN 08998418. doi: 10.1002/joc.612. URL [https://onlinelibrary.](https://onlinelibrary.wiley.com/doi/full/10.1002/joc.612)
617 [wiley.com/doi/full/10.1002/joc.612](https://onlinelibrary.wiley.com/doi/full/10.1002/joc.612). Publisher: John Wiley & Sons, Ltd.

618 T. G. Shepherd. The dynamics of temperature extremes. *Nature*, 522(7557):425–427, June 2015.
619 ISSN 0028-0836, 1476-4687. doi: 10.1038/522425a. URL [http://www.nature.com/articles/](http://www.nature.com/articles/522425a)
620 [522425a](http://www.nature.com/articles/522425a).

- 621 J. Sillmann, T. G. Shepherd, B. van den Hurk, W. Hazeleger, O. Martius, J. Slingo, and J. Zscheis-
622 chler. Event-Based Storylines to Address Climate Risk. *Earth's Future*, 9(2):e2020EF001783, Feb.
623 2021. ISSN 2328-4277. doi: 10.1029/2020EF001783. URL [https://onlinelibrary.wiley.com/
624 doi/full/10.1029/2020EF001783](https://onlinelibrary.wiley.com/doi/full/10.1029/2020EF001783). Publisher: John Wiley & Sons, Ltd.
- 625 E. T. Smith and S. C. Sheridan. The influence of extreme cold events on mortality in the United
626 States. *Science of The Total Environment*, 647:342–351, Jan. 2019. ISSN 0048-9697. doi: 10.
627 1016/j.scitotenv.2018.07.466. URL [https://www.sciencedirect.com/science/article/pii/
628 S0048969718329619](https://www.sciencedirect.com/science/article/pii/S0048969718329619).
- 629 E. T. Smith and S. C. Sheridan. Where Do Cold Air Outbreaks Occur, and How Have They
630 Changed Over Time? *Geophysical Research Letters*, 47(13):e2020GL086983, 2020. ISSN 1944-
631 8007. doi: 10.1029/2020GL086983. URL [https://onlinelibrary.wiley.com/doi/abs/10.
632 1029/2020GL086983](https://onlinelibrary.wiley.com/doi/abs/10.1029/2020GL086983). eprint: <https://onlinelibrary.wiley.com/doi/pdf/10.1029/2020GL086983>.
- 633 M. Trnka, J. E. Olesen, K. C. Kersebaum, A. O. Skjelvåg, J. Eitzinger, B. Seguin, P. Peltonen-
634 Sainio, R. Rötter, A. Iglesias, S. Orlandini, M. Dubrovský, P. Hlavinka, J. Balek, H. Eckersten,
635 E. Cloppet, P. Calanca, A. Gobin, V. Vučetić, P. Nejedlik, S. Kumar, B. Lalic, A. Mestre, F. Rossi,
636 J. Kozyra, V. Alexandrov, D. Semerádová, and Z. Žalud. Agroclimatic conditions in Europe
637 under climate change. *Global Change Biology*, 17(7):2298–2318, 2011. ISSN 1365-2486. doi: 10.
638 1111/j.1365-2486.2011.02396.x. URL [https://onlinelibrary.wiley.com/doi/abs/10.1111/
639 j.1365-2486.2011.02396.x](https://onlinelibrary.wiley.com/doi/abs/10.1111/j.1365-2486.2011.02396.x). eprint: [https://onlinelibrary.wiley.com/doi/pdf/10.1111/j.1365-
640 2486.2011.02396.x](https://onlinelibrary.wiley.com/doi/pdf/10.1111/j.1365-2486.2011.02396.x).
- 641 K. Van Der Wiel, H. C. Bloomfield, R. W. Lee, L. P. Stoop, R. Blackport, J. A. Screen, and F. M.
642 Selten. The influence of weather regimes on European renewable energy production and demand.
643 *Environmental Research Letters*, 14(9), 2019. ISSN 17489326. doi: 10.1088/1748-9326/ab38d3.
644 URL <https://doi.org/10.1088/1748-9326/ab38d3>.
- 645 G. J. Van Oldenborgh, E. Mitchell-Larson, G. A. Vecchi, H. De Vries, R. Vautard, and F. Otto. Cold
646 waves are getting milder in the northern midlatitudes. *Environmental Research Letters*, 14(11):
647 114004, Oct. 2019. ISSN 17489326. doi: 10.1088/1748-9326/ab4867. URL [https://iopscience.
648 iop.org/article/10.1088/1748-9326/ab4867](https://iopscience.iop.org/article/10.1088/1748-9326/ab4867). Publisher: IOP Publishing.
- 649 S. J. Vavrus. The Influence of Arctic Amplification on Mid-latitude Weather and Climate.

- 650 *Current Climate Change Reports*, 4(3):238–249, Sept. 2018. ISSN 2198-6061. doi: 10.1007/
651 s40641-018-0105-2. URL <https://doi.org/10.1007/s40641-018-0105-2>.
- 652 E. Vogel, M. G. Donat, L. V. Alexander, M. Meinshausen, D. K. Ray, D. Karoly, N. Meinshausen,
653 and K. Frieler. The effects of climate extremes on global agricultural yields. *Environmental*
654 *Research Letters*, 14(5):054010, May 2019. ISSN 1748-9326. doi: 10.1088/1748-9326/ab154b.
655 URL <https://dx.doi.org/10.1088/1748-9326/ab154b>. Publisher: IOP Publishing.
- 656 P. Yiou. AnaWEGE: A weather generator based on analogues of atmospheric circulation.
657 *Geoscientific Model Development*, 7(2):531–543, 2014. ISSN 19919603. doi: 10.5194/
658 gmd-7-531-2014. URL [https://www.researchgate.net/publication/260633068_AnaWEGE_A_](https://www.researchgate.net/publication/260633068_AnaWEGE_A_weather_generator_based_on_analogues_of_atmospheric_circulation)
659 [weather_generator_based_on_analogues_of_atmospheric_circulation](https://www.researchgate.net/publication/260633068_AnaWEGE_A_weather_generator_based_on_analogues_of_atmospheric_circulation).
- 660 P. Yiou and C. Déandréis. Stochastic ensemble climate forecast with an analogue model. *Geo-*
661 *scientific Model Development*, 12(2):723–734, Feb. 2019. ISSN 19919603. doi: 10.5194/
662 gmd-12-723-2019. Publisher: Copernicus GmbH.
- 663 P. Yiou and A. Jézéquel. Simulation of extreme heat waves with empirical importance sampling.
664 *Geoscientific Model Development*, 13(2):763–781, Feb. 2020. ISSN 19919603. doi: 10.5194/
665 gmd-13-763-2020. Publisher: Copernicus GmbH.
- 666 P. Yiou and M. Nogaj. Extreme climatic events and weather regimes over the North Atlantic:
667 When and where? *Geophysical Research Letters*, 31(7), Apr. 2004. ISSN 00948276. doi: 10.1029/
668 2003GL019119. URL <https://onlinelibrary.wiley.com/doi/full/10.1029/2003GL019119>.
669 Publisher: John Wiley & Sons, Ltd.